Invest Clin 67(1): 73 - 91, 2026 https://doi.org/10.54817/IC.v67n1a06

Withaferin-A induces apoptosis and autophagy in colorectal cancer cell lines via down-regulated expression of histone deacetylase 1.

Qiong Wang[1,2] *and Caixia Li*[3]

[1]Qilu Hospital of Shandong University, Jinan, Shandong, China.
[2]Endoscopy Center, Weifang NO.2 People's Hospital, Weifang, Shandong, China.
[3]Department of Stomatology, Shandong Provincial People's Hospital, Jinan, Shandong, China.

Keywords: Apoptosis; Autophagy; Histone Deacetylase 1; Aberrant Crypt Foci; Chemoprevention.

Abstract. Colorectal cancer (CRC) remains the third most common malignancy worldwide, and there is an urgent need for low-toxicity, mechanism-based preventives or adjuvants. Withaferin-A (WA), a plant-derived steroidal lactone, exhibits broad antitumor activity; however, its role in CRC and its interactions with epigenetic regulators, such as histone deacetylase 1 (HDAC1), remain unclear. Therefore, we investigated whether WA suppresses CRC growth by down-regulating HDAC1 while inducing apoptosis and autophagy. Caco2 and HT-29 cells were treated with 0–5 μM WA; viability, colony formation, and migration decreased significantly (IC_{50} 0.70–1.52 μM). Techniques such as Annexin-V/7-AAD flow cytometry, MDC staining, TEM, and LC3B immunofluorescence showed that 1 μM WA notably increased apoptosis and autophagic flux, along with reduced HDAC1 and p62 levels, higher LC3B-II/I ratios, and an increased Bax/Bcl-2 ratio. Overexpression of HDAC1 via a lentiviral vector reversed these effects, confirming dependence on HDAC1. For translational relevance, eight-week-old C57BL/6J mice were first exposed to the food-borne carcinogen IQ (2-amino-3-methyl-3H-imidazo[4,5-f]quinoline, 100 mg/kg) every other day for three weeks to induce aberrant crypt foci (ACF). Starting the day after the first IQ dose, animals received WA (2 mg/kg) or vehicle (corn oil) by gavage every other day for the same period. WA reduced the number of macroscopic ACF by more than 60%, restored HDAC1-related LC3B and p62 expression to normal levels, and showed no toxicity based on body weight or general health assessments. These findings suggest that WA provides potent, low-toxicity chemopreventive effects against CRC lesion formation through HDAC1-dependent induction of apoptosis and autophagy, supporting its further consideration as a preventive or adjuvant agent.

Corresponding author: Qiong Wang. Endoscopy Center. Qilu Hospital of Shandong University. 107 Wenhuaxi Road, Jinan, Shandong 250012, China. Tel: +86 13563606469. Email: Wangqiong7979@163.com

La withaferina-A induce la apoptosis y la autofagia en líneas celulares de cáncer colorrectal mediante la regulación negativa de la expresión de la histona deacetilasa 1.

Invest Clin 2026; 67 (1): 73 – 91

Palabras clave: Apoptosis; Autofagia; Histona Desacetilasa 1; Focos de Criptas Aberrantes; Quimioprevención.

Resumen. El cáncer colorrectal (CCR) sigue siendo la tercera malignidad más común en todo el mundo, y existe una necesidad urgente de preventivos o adyuvantes de baja toxicidad basados en mecanismos. Withaferin-A (WA), una lactona esteroide derivada de plantas, ha mostrado una amplia actividad antitumoral, pero su papel en el CRC y su interacción con reguladores epigenéticos, como la histona deacetilasa 1 (HDAC1), no están claros. Por lo tanto, se evaluó si WA suprime el crecimiento de CRC al regular la actividad de HDAC1 hacia abajo e inducir concomitantemente apoptosis y autofagia. Las células Caco2 y HT-29 se expusieron a WA 0–5 μM; la viabilidad, la formación de colonias y la migración se inhibieron marcadamente (IC_{50} 0.70–1.52 μM). La citometría de flujo con Annexin-V/7-AAD, la tinción con MDC, la inmunofluorescencia de TEM y de LC3B mostraron que WA a 1 μM aumentó significativamente la apoptosis y el flujo autofágico, acompañados de la regulación descendente de HDAC1 y p62, la regulación ascendente de LC3B-II/I y un aumento en la relación Bax/Bcl-2. La sobreexpresión de HDAC1 mediada por lentivirus revertió todos estos efectos, lo que confirma la dependencia de HDAC1. Para evaluar la relevancia traslacional, a ratones C57BL/6J de ocho semanas de edad se les administró primero el carcinógeno el carcinógeno de origen alimentario, 2-amino, 2-amino-3-metil-3H-imidazo[4,5-f]quinoline (100 mg/kg), cada dos días durante 3 semanas, para inducir focos de cripta aberrantes (ACF). A partir del día siguiente a la primera dosis de carcinógeno, los animales recibieron, adicionalmente, WA (2 mg/kg) o vehículo (aceite de maíz) por gavage cada dos días durante el mismo período. WA redujo el número macroscópico de ACF en más del 60%, restableció la expresión de LC3B y p62 asociada a HDAC1 a niveles normales y no mostró toxicidad ni en el peso corporal ni en el monitoreo general de la salud. Estos datos indican que WA ejerce una quimioprevención potente y de baja toxicidad contra la formación de lesiones de CRC mediante la inducción de apoptosis y autofagia dependientes de HDAC1, lo que respalda su desarrollo adicional como agente preventivo o adyuvante.

Received: 15-10-2025 Accepted: 21-12-2025

INTRODUCTION

Colorectal cancer (CRC) is the third most diagnosed malignancy and the second leading cause of cancer-related death worldwide [1]. Despite advances in surgery, radiotherapy, and targeted agents, the 5-year survival rate of patients with advanced CRC remains below 20%, largely because of chemo-resistance and dose-limiting toxicities [2]. Therefore, the development of low-toxicity, mechanism-based preventive or adjuvant therapies is urgently needed.

Plant-derived small molecules have gained prominence due to their widespread antitumor effects and favorable safety profiles [3]. Withaferin-A (WA), a steroidal lactone derived from *Withania somnifera*, has demonstrated potent antiproliferative, proapoptotic, and antimetastatic effects across various solid tumors [4-6]. These effects are linked to proteasome inhibition, reactive oxygen species production, and modulation of key cancer-related signaling pathways, including STAT3 and NF-κB [7–9]. However, the role of WA in CRC and the exact molecular mechanisms underlying its activity remain incompletely understood.

An increasing body of evidence suggests that epigenetic dysregulation—especially abnormal histone acetylation—plays a key role in CRC initiation and progression[10,11]. Histone deacetylases (HDACs) remove acetyl groups, thereby repressing tumor-suppressor genes, and HDAC1 is often overexpressed in CRC tissues [12,13]. Small-molecule HDAC inhibitors (e.g., Trichostatin A) can restore acetylation balance and induce growth arrest or apoptosis, but their clinical use is limited by systemic toxicity [14]. Whether WA affects HDAC activity in CRC remains unexplored.

The present study, therefore, aimed to evaluate the anti-proliferative, pro-apoptotic, and anti-migratory effects of WA in human CRC cell lines and to determine whether these effects are mediated by downregulation of HDAC1-dependent epigenetic mechanisms. To assess translational relevance, we also examined WA activity in a murine model of colitis-associated CRC.

MATERIALS AND METHODS

Cell lines and culture conditions

Caco2 and HT-29 human CRC cells were obtained from Shanghai ZhongQiao Xin Zhou Biotechnology Co., Ltd. They were grown as monolayers in Dulbecco's Modified Eagle Medium (DMEM) (Gibco; Thermo Fisher Scientific, Inc.). The human CRC cell lines were supplemented with 10% fetal bovine serum (FBS, Biological Industries, Israel) and 1% penicillin/streptomycin (PEN/STREP 100×, MILLIPORE, USA). Cells were cultured in a humidified incubator at 37°C in 5% CO_2. The culture medium, including any treatments, was replaced every 48 hours. All treatments and controls contained a final dimethyl sulfoxide (DMSO, D2650, Sigma-Aldrich, USA) concentration of less than 0.1%.

Cell Counting Kit-8 (CCK8) assay

We used the CCK8 kit (K1018-5; APExBIO, USA) to detect cell viability. A total of 5×10^3 cells in 100 μL per well were cultured in five replicate wells of a 96-well plate in medium containing 10% FBS and allowed to adhere overnight. Then, the cells were treated with various concentrations of WA (W4394-5mg, Sigma-Aldrich, Saint Louis, MO, USA) (0, 0.5, 1, 2, 3, 4, 5 μM) for 24 and 48 hours. WA was diluted in 0.1% DMSO. Control cells were treated with 0.1% DMSO in culture medium. Following the manufacturer's instructions, 10 μL of CCK8 reagent was added to 90 μL of DMEM to prepare a working solution, which was then incubated for 30 minutes at 37°C. 100 μL of the working solution was added to each well. The absorbance (OD) was measured at 450 nm using a microplate spectrophotometer (Varioskan Flash 4.0, Thermo Fisher Scientific, Waltham, MA, USA). All experiments were performed in quintuplicate, with five wells per replicate. The viability rate was calculated as: (OD test – OD blank) / (OD control – OD blank) × 100%. The OD blank consisted of wells with 0.1% DMSO in culture medium. The half-maximal inhibitory concentration (IC_{50}) values were determined using GraphPad 8.0. Subsequently, cells were treated in complete medium with or without 1 μM WA for future experiments.

Colony formation assay

CRC cells were seeded into 6-well plates at a density of 1000 cells per well and cultured with 0 or 1 μM WA. They were incubated at 37°C for 14 days to allow colony for-

mation. Finally, the cells were washed with phosphate-buffered saline (PBS), fixed in methanol at room temperature for 30 minutes, washed again with PBS, and stained with 0.1% crystal violet at room temperature for 30 minutes. After washing with PBS, the wells were photographed with a smartphone camera (VIVO X6 PLUS, China), and colonies with at least 50 cells were visually counted and quantified.

Wound healing assay

Wound-healing assays were performed to evaluate CRC cell motility. CRC cells were seeded in 6–well plates at a density of 1×10^6 cells per well. After 24 h, the cell monolayer was scratched with a 10μL pipette tip. The wound-healing assay was performed in monolayer culture, after which the cells were cultured in serum–free medium. Wounds were washed with PBS and incubated in serum-free medium in the presence of 0 or 1 μM WA. Images were captured at different timepoints (0, 24 and 48 h). The wound-healing area was calculated using ImageJ software (version 1.8.0.112; National Institutes of Health).

Transwell (Migration) assay

Migration ability was evaluated using 24-well Transwell chambers (8.0 μm pore size; 3422, Corning Costar, USA). After 48 hours of treatment with the respective agents, CRC cells were digested and suspended in FBS-free medium. Subsequently, 1×10^5 cells were allowed to migrate from the upper chamber, which contained 200 μL of medium without FBS, to the lower chamber, which contained 700 μL of medium with 30% FBS. After incubating the Transwells for 24 hours, non-invading cells in the upper chamber were removed with a cotton swab, and cells that had invaded the membrane were fixed in methanol for 5 minutes and stained with crystal violet for 30 minutes. The cells that migrated through the polycarbonate membrane were counted under a Nikon Ti-E inverted microscope (5 random fields per well, magnification ×100).

Analysis of apoptosis by Flow Cytometry (FCM)

CRC cells were cultured in 60 mm dishes at a density of 1×10^6 cells per well and treated with drugs for 24 hours as previously described. An Annexin V-APC/7-AAD apoptosis detection kit was used to assess cell morphology and apoptosis. Following the manufacturer's instructions, cells were washed twice with cold PBS, then collected and resuspended in 1× Annexin V Binding Buffer. Next, 5 μL of Annexin V-APC conjugate and 5 μL of 7-AAD solution were added to the cell suspension, which was incubated for 15 minutes at 2-8°C in the dark. Afterward, 400 μL of 1× Annexin V Binding Buffer was added to each tube. The samples were analyzed by flow cytometry using a CytoFLEX Flow Cytometer (Beckman Coulter, Inc., USA) within 1 hour of staining. Data were analyzed with CytExpert software.

Monodansylcadaverine (MDC) staining

MDC, an electrophoretic marker of autophagosome formation, was used to quantify autophagy induction. The autofluorescent drug MDC is a selective marker for acidic vesicular organelles (AVOs), such as autophagic vacuoles and autolysosomes. The effects of WA and the control group on autophagy levels in CRC cells were assessed using the MDC method. Normal cells displayed a uniform yellow-green stain, while autophagosomes appeared as densely packed green granules of varying sizes, producing punctate green fluorescence. In brief, after the specified treatment conditions, cells were seeded into a 6-well plate (3×10^6 cells/well) and cultured overnight until reaching 50–60% confluence. As described above, they were divided into two groups for different interventions. At the designated time points, the original medium was removed, cells were washed with 1× wash buffer (diluted in deionized water), incubated with the prepared MDC staining solution at room temperature for 45 minutes in the dark, and then washed three times with 1× wash buffer. Fluores-

cent images were captured using an inverted fluorescence microscope (magnification ×200) (Nikon Microscope, Tokyo, Japan) at an excitation wavelength of 355 nm and an emission filter of 512 nm (Leica, Wetzlar, Germany).

Ultra-structures observed by transmission electron microscopy

To evaluate the effect of WA on cell autophagy in CRC cells, cells were treated with or without WA (1 μM) for 48 hours. The cells were then washed with PBS, collected by centrifugation at 1,000 × g (Eppendorf, Hamburg, Germany), and fixed in cold (4°C) 2.5% glutaraldehyde solution (Servicebio Technology Co., Ltd., Wuhan) for 1 hour. The specimens were subsequently rinsed with 0.1 mL PBS, embedded in agarose for pre-embedding, postfixed in 1% osmium tetroxide (Ted Pella Inc., California, USA) in the dark for 2 hours at room temperature, dehydrated through a graded series of ethanol solutions (30-100%) and two changes of acetone (Sinaopharm Group Chemical Reagent Co., Ltd.), and then infiltrated with EMBed 812 (SPI, USA) for resin penetration and embedding. After polymerization, the resin blocks were sectioned at 60–80 nm on a Leica UC7 ultramicrotome (Leica, Wetzlar, Germany), and the tissues were transferred onto 150-mesh copper grids coated with Formvar film. Copper grids were stained with 2% uranyl acetate in saturated alcohol for 8 minutes, then with 2.6% lead citrate for 8 minutes, with light exposure avoided during staining. The grids were placed on the grid board and dried overnight at room temperature. Representative areas were examined with an HT7800 transmission electron microscope (Hitachi Ltd., Tokyo, Japan).

Immunofluorescence Assay

To further confirm that autophagy was induced by WA, CRC cells were seeded into 24-well cell culture plates at a density of 1.5×10^5 cells per well. The cells were divided into two groups as previously described. After fixing with 4% paraformaldehyde, the cells were permeabilized with 0.3% Triton X-100 for 5 minutes and blocked with 5% normal goat serum for 1 hour. The cells were then incubated with rabbit anti-LC3A/B primary antibody (1:200) overnight at 4°C. After washing with PBS, the cells were immunostained with FITC-conjugated goat anti-rabbit secondary antibody (1:100) for 1 hour at room temperature in the dark. Next, the cell nuclei were stained with 4',6-diamidino-2-phenylindole (DAPI) for 3 minutes. Finally, immunofluorescence images were captured and observed using a fluorescence microscope (magnification, ×400). The Dylight 488, Goat Anti-Rabbit IgG (cat. no. A23220; 1:500) was obtained from Abbkine Scientific Co., Ltd., Wuhan, China.

RNA extraction, Reverse Transcription, and RT-qPCR

CRC cells were treated with 1 μM WA for the indicated duration (48 hours) and harvested using TRIzol reagent (Invitrogen, Thermo Fisher Scientific, Inc.). After adding 1/5 volume of chloroform (Invitrogen, Thermo Fisher Scientific, Inc.), the mixture was centrifuged at 12000g for 15 minutes at 4°C, and the supernatants were transferred to new, clear centrifuge tubes. An equal volume of isopropanol was added to each supernatant and gently mixed. After incubation at room temperature for 30 minutes, the mixture was centrifuged at 12000g for 15 minutes. The pellets were washed once with 75% ethanol and dissolved in RNase-free water at an appropriate volume. Following RNA quantification, reverse transcription (RT) reactions were performed to convert total RNA into cDNA using the SureScript™ First-Strand cDNA Synthesis Kit (cat. no. QP056, GeneCopoeia, Inc., Guangzhou, China) and reverse transcriptase (Takara, Tokyo, Japan) according to the manufacturer's protocol. Cycling parameters were set at 95°C for 30 seconds (denaturation), 95°C for 5 seconds (annealing), and 60°C for 34 seconds (extension), with 40 cycles performed.

The gene-specific primer sequences, synthesized by Generay Biotech Co., Ltd. (Shanghai, China) and derived from PrimerBank, are summarized in Supplemental Table 1. GAPDH was used as an internal control to normalize RNA quantity and quality across samples. The presence of HDAC1, Bax, Bcl-2, p62, and LC3B transcripts was analyzed by Quantitative RT-qPCR (10-μL reaction volume) using the BlazeTaq™ SYBR® Green qPCR Mix 2.0 Kit (cat. no. QP031, GeneCopoeia, Inc., Guangzhou, China). Real-time reverse transcription quantitative PCR (RT-qPCR) was performed on an Applied Biosystems 7500 system according to the manufacturer's instructions. Data were analyzed using the $2^{-\Delta\Delta Cq}$ method, with relative quantification calculated by the formula $2^{-\Delta\Delta Ct}$, where $\Delta Ct = Ct$ of target gene $- Ct$ of GAPDH, and $\Delta\Delta Ct = \Delta Ct$ of treatment $- \Delta Ct$ of control.

Supplemental Table 1. Primers for RT-qPCR.

Gene		Primer sequence, 5'3'
GAPDH	F	GGACCTGACCTGCCGTCTAG
	R	GTAGCCCAGGATGCCCTTGA
Bax	F	CCCGAGAGGTCTTTTTCCGAG
	R	CCAGCCCATGATGGTTCTGAT
Bcl-2	F	GGTGGGGTCATGTGTGTGG
	R	CGGTTCAGGTACTCAGTCATCC
LC3B	F	AAGGCGCTTACAGCTCAATG
	R	CTGGGAGGCATAGACCATGT
HDAC1	F	CGCCCTCACAAAGCCAATG
	R	CTGCTTGCTGTACTCCGACA
p62	F	GACTACGACTTGTGTAGCGTC
	R	AGTGTCCGTGTTTCACCTTCC

F, forward; R, reverse.

Western blotting

Western blotting was performed to assess protein expression levels of the anti-apoptotic Bcl-2 and the pro-apoptotic Bax; the autophagic markers LC3 II/I and p62; and HDAC1. After the specified drug treatments, total protein was extracted from CRC cells at 48 hours. The cells were washed twice with ice-cold PBS and lysed in complete cell lysis buffer (50 mM Tris- HCl, pH 7. 4, 7.4,150 mM NaCl, 1% Triton X- 100, 0. 25% Na-Deoxycholate,1 mM EDTA, 1 mM NaF, 1 mM dithiothreitol, 1 mM PMSF,1 mM activated Na 3 VO 4, 0.02 μM aprotinin, 0. 16 μM leupeptin, and 0.22 μM pepstatin). Protein extracts were heated at 99°C for 5 minutes and then cooled on ice. Protein concentrations were measured using a BCA protein assay kit (Tiangen Biotech Co., Ltd.). Equal amounts (30 μg) of protein from each sample were loaded and separated on a 10% SDS-PAGE gel through 6–12% gels, then transferred onto PVDF membranes (Millipore, USA). The membranes were blocked in rapid sealing fluid for 30 minutes, then incubated overnight at 4°C with primary antibodies. The blots were washed three times for 5 minutes with TBST, then incubated with specific secondary antibodies at room temperature for 1 hour. After washing three additional times for 5 minutes in TBST, the bands were visualized with an ECL detection reagent, quantified using ImageJ, and normalized to GAPDH as the endogenous control. The antibody information is as follows: GAPDH (product no. 5174; 1: 1000 dilution), LC 3 A/B (product no. 12741; 1: 1000 dilution), and HDAC 1 (product no. 34589; 1: 1000 dilution) from Cell Signaling Technology; p 62 (cat. no. ab 109012; 1: 2000 dilution) and Bax (cat. no. ab 182733; 1: 2000 dilution) from Abcam; Bcl- 2 (cat. no. SC 271268; 1: 200 dilution) from Santa Cruz Biotechnology. Goat anti- Rabbit IgG-HRP (cat. no. HA 1001; 1: 10, 000 dilution) and Goat anti- Mouse IgG- HRP (cat. no. HA 1006; 1: 5000 dilution) from Huaan Biotechnology, Co., Ltd. (Hangzhou, China). The secondary antibody diluent buffer (P 0023 D- 100 mL) was obtained from Beyotime Biotechnology (Shanghai, China).

Separation of the nucleus from the cytoplasm

A nucleoprotein extraction kit was used to separate the nucleus from the cytoplasm

according to the manufacturer's protocol. The CRC cells were washed three times with cold PBS and collected into 1.5 mL Eppendorf tubes using a cell scraper. Cells were centrifuged at 500 × g for 3 minutes at 4°C, and the supernatants were discarded. Cell lysates were added to the precipitates. The Eppendorf tubes were then vortexed for 15 seconds at 5-minute intervals, for a total of 3 cycles. Next, the suspensions were centrifuged for 5 minutes at 12,000 × g, and the supernatants were collected as the cytoplasmic fraction. The nuclear lysates were added to the precipitates. After vortexing for 15 seconds every 10 minutes for a total of 4 times, the suspensions were centrifuged for 10 minutes at 12,000 x g, and the supernatants contained the cytoplasmic proteins. Finally, the samples were packaged and stored at -80°C for future use.

Histone acetyltransferase activity/ inhibition assay

Trichostatin A (TSA) is a specific inhibitor of HDACs, and its inhibitory ability has been validated in many experiments. Cells were divided into three groups: control, WA, and TSA. The control and WA groups were treated with medium containing or lacking WA, respectively. The TSA group cells were pretreated with the inhibitor TSA. Nuclear extracts were prepared as described above, and the EpiQuik™ HDAC Activity/Inhibition Kit (Colorimetric) (P-4002) (Epigentek Group Inc.) was used to determine whether WA can inhibit HDACs in CRC cells similarly to TSA. The assay was carried out according to the provided protocol. Activity was expressed as relative OD values per mg protein (OD/mg), based on triplicate measurements (n=4). HDAC activity/inhibition assays were performed either with or without HDAC inhibitors (HDACi). The inhibitory rate (%) was calculated as: {1 - [OD (control – blank) – OD (inhibitor sample – blank)] / [OD (control – blank) – OD (no inhibitor sample – blank)]} × 100%.

Lentivirus-mediated RNA interference

Lentiviral particles and Polybrene were purchased from Shanghai Genechem Co., Ltd. The overexpressed gene was named LV-HDAC1 (14721-1), and the negative control (NC) was labeled as CON238. The procedure was as follows: CRC cells were seeded in 6-well plates at a density of 1×10^5 cells per well. Lentiviral particles with a multiplicity of infection of 10 for HT-29 and 18 for Caco2 were added to the cells. GFP-expressing cells were observed using fluorescence microscopy, and stable transfected cells were selected with puromycin (8 μg/mL). After RNA and protein were collected, and the interference efficiency was calculated, the cells were used for subsequent experiments. Levels of HDAC1 mRNA and protein expression were measured by RT-qPCR and Western blotting. Previous research has shown that HDAC1 expression decreases upon WA treatment. It was hypothesized that WA-induced apoptosis and autophagy in CRC cells were mediated by HDAC1 downregulation. CRC cells transfected with PCMV-HDAC1 or PCMV-NC were treated with 1 μM WA for subsequent experiments, including colony formation, scratch healing, Transwell migration, flow cytometry, Western blotting, and RT-qPCR assays, to verify that WA-induced apoptosis and autophagy were mediated by HDAC1 downregulation.

Studies *in vivo*

Eight-week-old C57BL/6J mice were purchased from SiPeiFu Biotechnology Co., Ltd., Beijing. They were housed under standard laboratory conditions. The animals were kept 3–5 per individually ventilated cage (IVC) under specific-pathogen-free (SPF) conditions at 22 ± 2°C, 40–60% relative humidity, and a 12- hour light/12- hour dark cycle (lights on from 07: 00 to 19: 00). Sterilized squirrel cages, feed (high- fat diet), bedding, and drinking water were regularly replaced. WA (cat. no. T 5687- 250 mg), used in mice, was obtained from Targetmol

Chemicals Inc. (Boston, USA). 2- amino- 3- methyl- 3 H- imidazo [4, 5- f] quinoline IQ was supplied by Toronto Research Chemicals Inc. (Canada). Corn oil was purchased from Jinlongyu, China. Mice were weighed, and their initial body weights were recorded before placement in the cage. Body weights were measured again after 3 weeks on a high- fat diet and prior to each oral (gavage) drug/oil administration. The oil group received 0.2 mL of oil; the IQ group received 100 mg/kg body weight; and the WA group received 2 mg/kg body weight, with both IQ and WA dissolved in corn oil, administered once every two days. Mice were euthanized by cervical dislocation. IQ, a potent heterocyclic aromatic amine (HAA) formed during high-temperature cooking of protein-rich foods, is classified by the International Agency for Research on Cancer as a Group 2A carcinogen. In rodents, oral gavage doses of IQ can rapidly induce DNA adduct formation, chronic inflammation, and result in aberrant crypt foci (ACF) within 3–4 weeks. Eight-week-old C57BL/6J mice (n = 5 per group) were acclimated for 1 week and then maintained on a high-fat diet (Research Diets D12492, 60% kcal from fat) to promote tumor development. Colitis-associated ACF was induced via gavage of IQ dissolved in corn oil at 100 mg/kg body weight (0. 0,1 mL/10 g). Successful induction was defined as having≥20 macroscopically visible ACF per colon, along with histologically confirmed dysplasia at necropsy in the IQ-alone group. Body weight: mice were weighed before being placed in the cage, and initial weights were recorded; body weights were also measured and recorded before each intragastric gavage. General health status, including activity, stool consistency, and rectal bleeding, was assessed daily. This project was approved by the Laboratory Animal Ethics and Welfare Committee of Shandong University Qilu College of Medicine (Approval number: 21099).

Bodies against HDAC1 (cat. no. 10197-1-AP, 1:500) and LC3B (cat. no. 14600-1-AP, 1:1000) used in IHC were obtained from Proteintech Biotechnology, Inc. (Wuhan, China). Colorectal tissues were fixed in 4% paraformaldehyde for 24 hours, dehydrated through graded ethanol, cleared in xylene, and embedded in paraffin. Sections 4 μm thick were cut on a rotary microtome, deparaffinized, rehydrated, and stained with hematoxylin for 5 minutes, followed by eosin for 2 minutes. After dehydration and mounting, whole-slide digital images were captured at 200× magnification. Aberrant crypt foci (ACF) were identified by two independent investigators blinded to treatment groups according to established morphological criteria. The percentage of ACF per colon was calculated. Antigen retrieval was performed by heating sections in 10 mM citrate buffer (pH 6.0) at 95°C for 20 minutes. Endogenous peroxidase activity was blocked with 3% H_2O_2 in methanol for 15 minutes, followed by 5% normal goat serum for 30 minutes. Sections were incubated overnight at 4°C with primary antibodies: rabbit anti-HDAC1 (Proteintech, 10197-1-AP, 1:500) and rabbit anti-LC3B (Proteintech, 14600-1-AP, 1:1000). After PBS washes, horseradish-peroxidase-conjugated goat anti-rabbit IgG (Huaan, HA1001, 1:200) was applied for 1 hour at room temperature. DAB was used as the chromogen; sections were counterstained with hematoxylin, dehydrated, and mounted. Five non-overlapping high-power fields (HPF, 400×) per section were photographed. Integrated optical density (IOD) of positive staining was measured using Image-Pro Plus 6.0 (Media Cybernetics). Data were normalized to the total tissue area in each field and expressed as IOD/μm^2. Mean values from five mice per group were used for statistical analysis.

Statistical analysis

GraphPad Prism 8.0.1 software was used for statistical analysis. The results are presented as mean ± SD (n≥3). Single-point data (e.g., IC_{50} values, apoptotic index, protein densitometry) were first tested for normality (Shapiro–Wilk test) and homoge-

neity of variances (Levene's test). Normally distributed data were compared between two groups using an unpaired Student's t-test or among three or more groups with one-way ANOVA followed by Tukey's post-hoc test. Repeated measurements (such as CCK-8 viability assays and body-weight curves) were analyzed with two-way repeated-measures ANOVA (factors: treatment and time), followed by Bonferroni's post-hoc test when an interaction was detected. The statistical significance of differences between groups ($p<0.05$) was assessed by one-way ANOVA.

RESULTS

Withaferin-A inhibits the proliferation and motility/migration of CRC cells

To evaluate the anticancer effect of WA on CRC cell lines, cells were treated with various concentrations of WA. The CCK8 assay revealed that WA significantly reduced cell viability in a dose- and time-dependent manner compared to the control group (Fig. 1A-C). The half maximal inhibitory concentration (IC_{50}) values are shown in Table 1. Next, the role of WA in colony formation was assessed. Compared to the control group, the number of colonies in the WA group was significantly decreased (Fig. 1D and E). Changes in the motility and migration capacity of CRC cells were examined using wound healing and Transwell (migration) assays. Decreased cell motility was observed in CRC cells treated with WA. The 48-hour wound-healing rate in the WA group differed significantly from that in the control group (Fig. 1F and G). Cell migration capacity was also reduced in the WA-treated group compared with the control. Additionally, the number of CRC cells migrating into the lower chamber differed significantly (Fig. 1H and I). These assay results indicate that cell proliferation, migration, and overall activity were significantly reduced in the WA group compared with the control group.

Withaferin-A induces the apoptosis of CRC cells

To confirm the effect of WA on cell apoptosis in CRC cells, cells treated with 0 and 1 μM of WA for 24 hours were analyzed by flow cytometry. The data showed significant differences in apoptosis rates among the CRC cells; all results are presented in (Fig. 1J and K). WA treatment increased apoptosis in CRC cells, which inhibits their growth.

Withaferin-A induces the autophagy of CRC cells

The results of MDC staining and TEM assays are shown in (Fig. 2A–D). The data indicate a significant difference in the number of autophagosomes between the two groups. As shown in the histogram, fluorescence intensity analysis revealed that autophagic vesicles in the WA group were significantly higher than in the control group. Additionally, LC3B fluorescence intensity indicated a significant difference in autophagy levels between the two groups (Fig. 2E and F).

Effect of Withaferin-A on HDAC1/LC3B / p62/Bax and Bcl-2 expression in CRC cells

RT-qPCR was used to measure the mRNA levels of LC3B, p62, Bax, and Bcl-2 in response to WA. As shown in (Fig. 3A - B), treatment with WA increased LC3B and Bax mRNA levels and decreased p62 and Bcl-2 mRNA levels. Western blotting was performed to detect the protein levels of these molecules, with or without 1 μM WA. The protein expression of HDAC1, p62, Bax, Bcl-2, and the LC3B II/I ratio, as previously described, is shown in (Fig. 3C and D). In summary, there were significant increases in LC3B II/I and the Bax to Bcl-2 ratio in the WA treatment group, alongside a reduction in p62 levels in total protein, as demonstrated in (Fig. 3E and F). The mRNA and total protein expression of HDAC1 were similarly decreased in the WA-treated group (Fig. 3G-I).

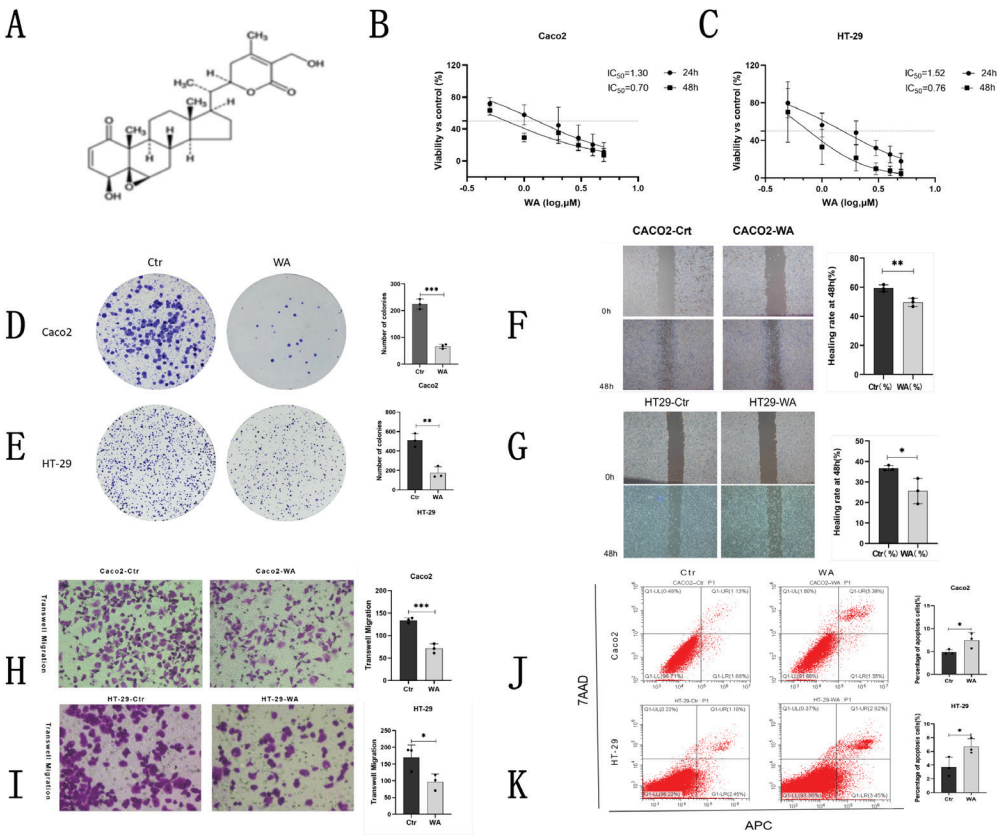

Fig. 1. The molecular structure of WA (A) and the CCK8 assay demonstrated that WA significantly decreased cell viability compared to the control group in a dose- and time-dependent manner. (B and C) IC_{50} values are provided in Table 1. The number of colonies in both groups was quantified, as shown in the graphs, and the corresponding histograms are included (D and E). Wound healing assay results and statistical graphs are shown in (F and G). The number of cells migrating into the lower chamber (H and I) was significantly different. Apoptosis rates in the two groups also showed significant differences (J and K). An unpaired Student's t-test was used, with n=3 replicates, * $p<0.05$, ** $p<0.01$, *** $p<0.001$. WA: Withaferin-A.

Table 1. IC_{50} of Withaferin-A in CRC Cells.

CRC Cells	IC_{50} of WA (μM)	
	24h	48h
CACO2	1.30	0.70
HT-29	1.52	0.76

CRC: colorectal cancer; WA: Withaferin-A. IC_{50}: half-maximal inhibitory concentration; CACO2: human colon adenocarcinoma-derived cell line; HT-29 human colorectal adenocarcinoma epithelial cell line.

Histone Acetyltransferase Activity/ Inhibition Assay

The HDAC Activity/Inhibition Assay demonstrated that WA can inhibit HDACs, similar to Trichostatin A (TSA), a specific HDAC inhibitor. The difference was statistically significant (Fig.4A). HDAC1 expression was notably increased after transfection with a lentiviral vector and purine screening. HDAC1 mRNA and protein levels were measured by RT-qPCR and Western blotting. The upregulation ratio also showed a significant difference (Fig.4B-D). Cell proliferation activity in the PCMV-HDAC1 group (HDAC1 overexpression) was significantly higher compared to the NC group (Fig.4E-H). The CCK8 assay determined the IC_{50} (Table 2) and revealed cell viability at various doses and time points relative to the control group. Additionally, cell motility and migration capacity increased in the PCMV-HDAC1 group (Fig.4I-L).

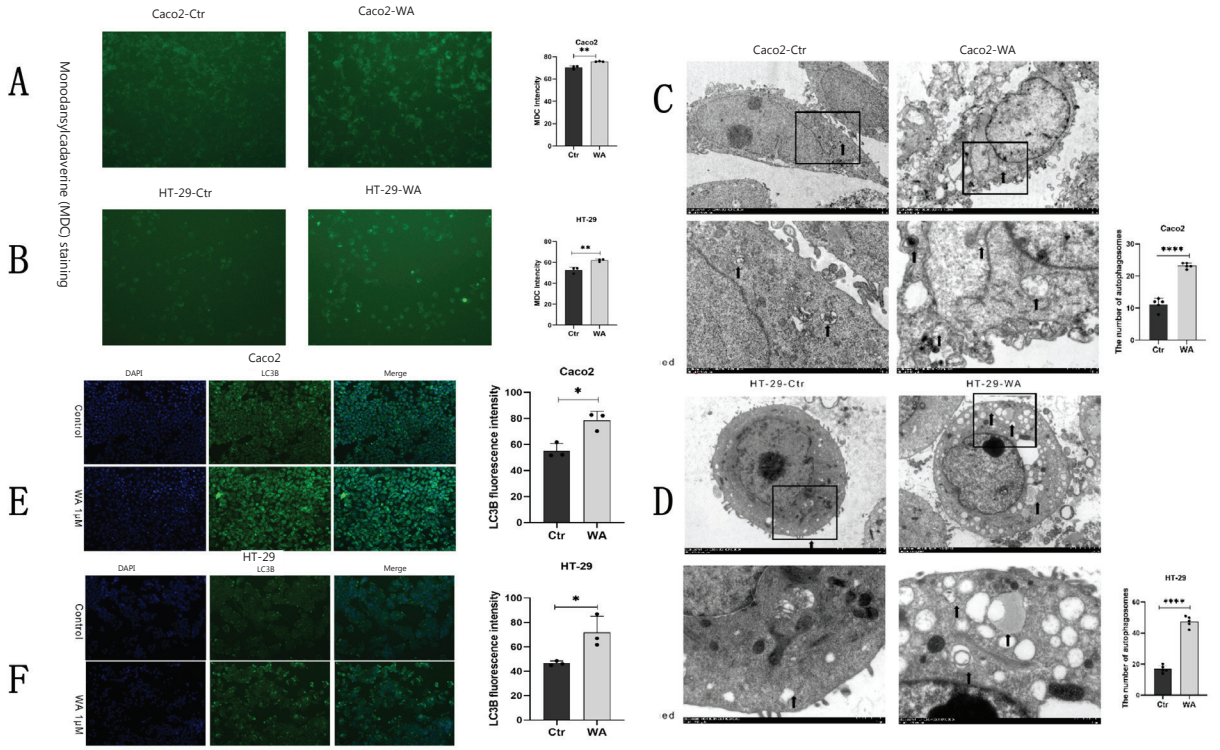

Fig. 2. Experiments using MDC staining were conducted to measure autophagosomes in two groups. Histograms indicated that autophagic vesicles in the WA group were significantly higher compared to the control group. (A-B) TEM analysis is displayed in (C). An enlarged section of the spectrogram (black box) is shown below (D). Autophagosome-like structures are marked with black arrows. Immunofluorescence analysis revealed that LC3B fluorescence intensity, an autophagy marker, varied significantly between the two groups (E and F). An unpaired Student's t-test was used, with n=3 replicates, * $p<0.05$, ** $p<0.01$, **** $p<0.0001$. WA: Withaferin-A; MDC: Monodansylcadaverine; TEM: Transmission Electron Microscope.

The apoptosis rates in the two groups

Flow cytometry analysis of apoptosis was also significantly reduced in the PCMV-HDAC1 group (Fig. 5A and B). Additionally, mRNA expression levels of molecules involved in apoptosis and autophagy were affected. Bax and LC3B expressions were notably decreased, while p62 and Bcl-2 were markedly increased in the PCMV-HDAC1 group (Fig. 5C and D). Protein expression levels of Bax/Bcl-2 and LC3B-II/I were significantly lower, whereas p62 levels were notably higher in the PCMV-HDAC1 group (Fig. 5E-H).

The study *in vivo*

Eight-week-old C57BL/6J mice were fed a high-fat diet for three weeks, then given the colonic carcinogen IQ (100 mg/kg) by gavage once every two days. Starting the day after, animals were gavaged every two days with either vehicle (corn oil) or Withaferin-A (WA, 2 mg/kg) dissolved in corn oil (Fig. 6A, B). Mice were weighed before being placed in the cage, and initial weights were recorded; body weight was also measured before each intragastric gavage. No significant differences were observed among groups at any time point, indicating that WA was well tolerated (Fig. 6C). After sacrifice, colons were excised longitudinally and examined. WA-treated mice showed a significant reduction in the number and size of macroscopically visible aberrant crypt foci (ACF) compared to the IQ-only group (Fig. 6D). HE staining

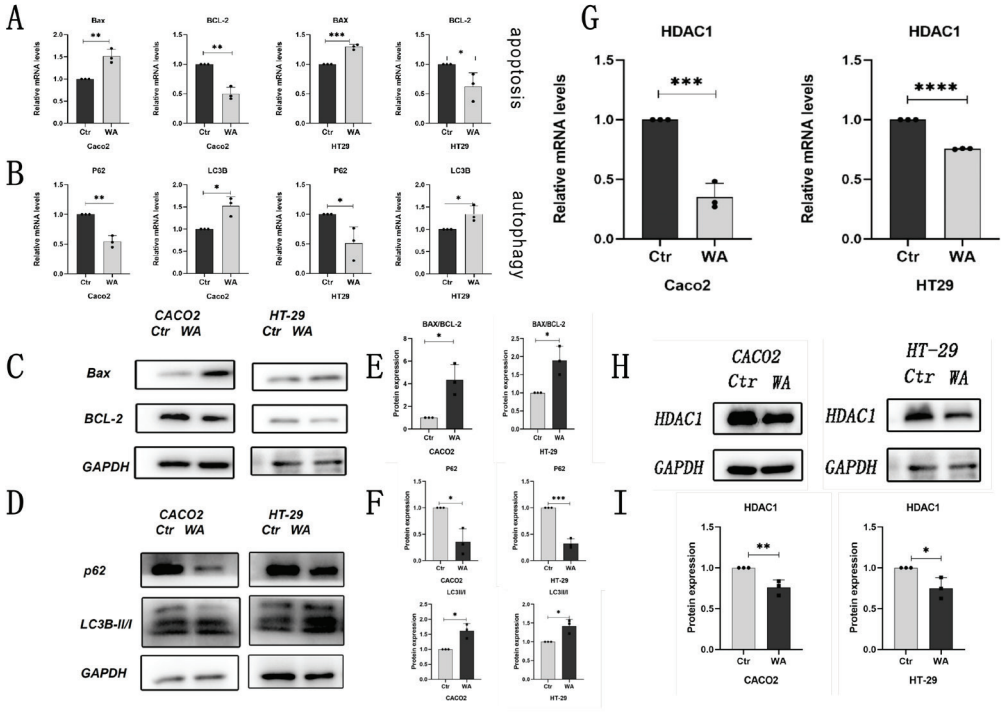

Fig. 3. Significant increases in LC3B/Bax and decreases in Bcl-2/p62 mRNA levels were observed, along with notable changes in protein expression of p62/Bax/Bcl-2 and the LC3B-II/I ratio, all of which were statistically significant. (C-F) RT-qPCR and Western blotting confirmed that HDAC1 mRNA and total protein levels were also significantly reduced in the W-treated group (G-I). An unpaired Student's t-test was used, with n=3 replicates, and significance levels indicated as * $p<0.05$, ** $p<0.01$, *** $p<0.001$, **** $p<0.0001$. WA: Withaferin-A; HDAC1: histone deacetylase 1.

Table 2. IC_{50} of **Withaferin-A** in CRC Cells.

CRC Cells	IC_{50} (WA=1uM)	
CACO2	PCMV-HDAC1	2.341
48h	PCMV-NC	1.738
HT-29	PCMV-HDAC1	3.239
48h	PCMV-NC	2.507

CRC: colorectal cancer; WA: Withaferin-A. IC_{50}: half-maximal inhibitory concentration; CACO2: human colon adenocarcinoma-derived cell line; HT-29 human colorectal adenocarcinoma epithelial cell line; HDAC1: Histone Deacetylase 1 enzyme; PCMV-HDAC1: CRC cells transfected with HDAC1; PCMV-NC: CRC cells not transfected with HDAC1.

was used to analyze the percentage of ACF. Colorectal tissue slices from all three groups were stained, revealing that ACF contained crypt branching, distortion, atrophy, surface irregularity, mucin depletion, Paneth cell metaplasia, cryptitis, crypt abscesses, basal plasmacytosis, or lymphoid aggregates, with statistical significance (Fig. 6E). Representative immunohistochemical images and quantitative analyses of LC3B and p62 expression from different groups are shown in (Fig. 6F). Compared to the IQ group, the WA group showed reduced LC3B and p62 positivity, indicating that WA can reduce the IQ-induced increase in LC3B and p62 expression (Fig. 6F).

DISCUSSION

Over the last few decades, the use of plant-derived edibles and the consumption of highly active, naturally occurring or synthetic, highly specific drugs have increased[15-18]. Plant-derived natural molecules have fewer side effects and are readily available. They have been used in the treatment of various

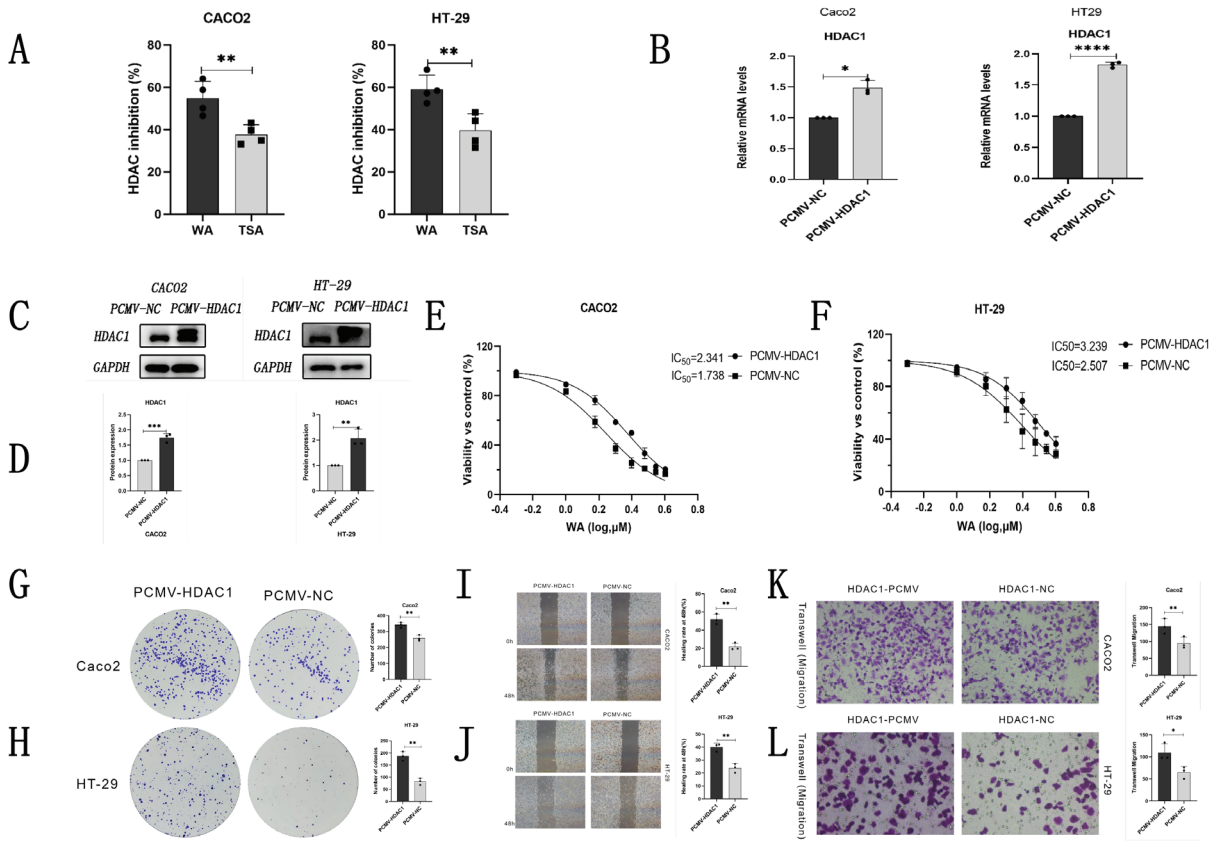

Fig. 4. The HDAC activity/Inhibition Assay showed that both WA and TSA decreased total HDAC mRNA levels, with the difference being statistically significant (A). HDAC1 mRNA and protein levels were measured by RT-qPCR and Western blotting, respectively, and the upregulation ratios indicated a statistically significant difference (B-D). The results of the CCK8 assay are presented in (E and F). The number of colonies for both groups, as shown in the graphs, was quantified and displayed in histograms (G and H). The wound-healing assay and its statistical analysis are shown in (I and J). The number of cells migrating into the lower chamber (K and L) differed significantly. An unpaired Student's t-test was used, with n≥3 replicates. Significance levels are indicated as * $p<0.05$, ** $p<0.01$, **** $p<0.0001$. WA: Withaferin-A; HDAC1: histone deacetylase 1; TSA: Trichostatin A.

diseases [19-21]. WA, a steroidal lactone, is a promising anticancer phytochemical that is abundantly isolated from Withania somnifera (a medicinal plant native to Asia) and exhibits anti-inflammatory, immunomodulatory, and anti-angiogenic properties[22, 23]. The potency of natural drugs or potential toxicity can often be addressed through semi-synthetic approaches. WA exerts its anti-tumorigenic effects in different types of cancer, especially in breast cancer [24].

Anticancer effect of WA contains its effects on cancer-relevant cellular processes (e.g., growth arrest, apoptosis induction, autophagy, metabolic adaptation, immune function, etc.) and molecular targets (e.g., suppression of oncogenes such as estrogen receptor-α, signal transducer and activator of transcription 3, etc.) [25, 26]. WA has promising roles in cancer prevention and therapy. It can reduce cellular proliferation and viability in certain cancer cell lines, modulate inflammatory pathways, and induce apoptosis, all of which have piqued interest in its use as a potential chemotherapeutic agent [27].

Some reported its ability to regulate epigenetic processes. However, acetylation has been studied infrequently, particularly

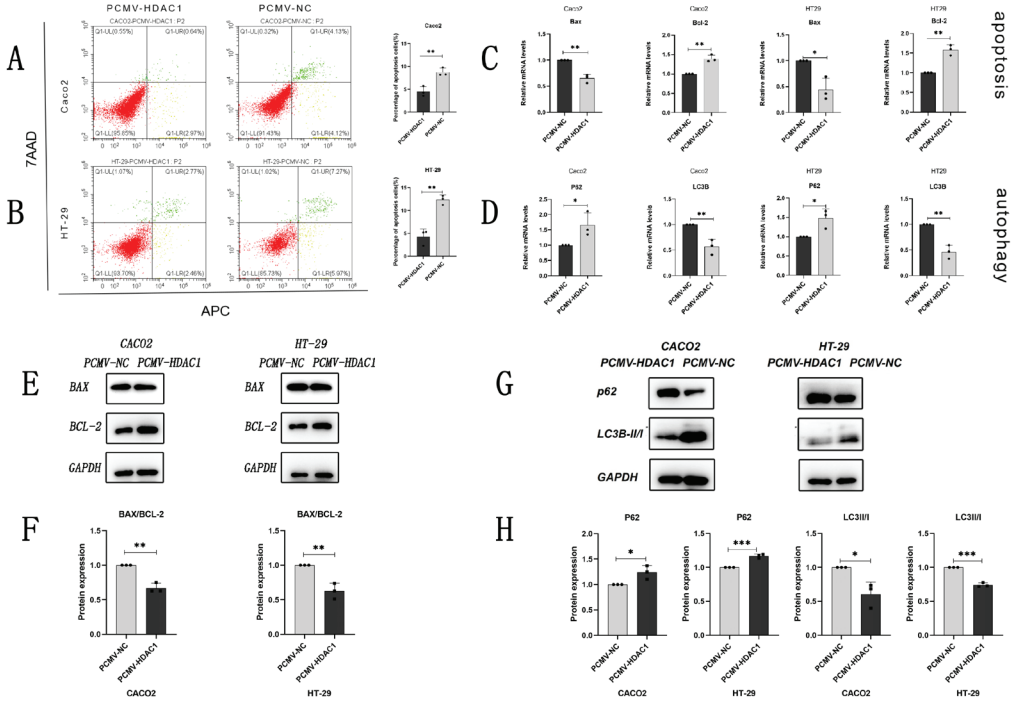

Fig. 5. The apoptosis rates between the two groups also differed significantly (A and B). RT-qPCR assay verified that the mRNA levels (C and D) of LC3B, Bax, Bcl-2, and p62 (E and F) are statistically significant. Western blotting confirmed the total protein expression of p62, LC3B-II/I, and Bax/Bcl-2 (G and H), with statistical significance (G and H). An unpaired Student's t-test was used, with n=3 replicates. * $p<0.05$, ** $p<0.01$, *** $p<0.001$.

in CRC cells. Histone acetylation is catalyzed by histone acetyltransferase (HAT) and HDACs. The goal of this study was to examine the anticancer effects of WA in CRC cells and to elucidate the mechanisms underlying its regulation of acetylation.

Firstly, cell proliferation and motility/migration in the WA group were significantly reduced compared to the control group. Secondly, WA induces apoptosis in CRC cells, with a significant increase in the Bax/Bcl-2 ratio at both the protein and mRNA levels. Thirdly, WA induces autophagy in CRC cells; p62 protein and mRNA expression were significantly decreased, while LC3B-II/I levels were significantly increased. Moreover, MDC staining and the TEC assay confirmed autophagy induction. Fourthly, the HDAC Activity Assay revealed that WA can inhibit HDAC activity, similar to Trichostatin A (TSA), a specific HDAC inhibitor. The differences were statistically significant. In this study, WA also increased the LC3B-II/I ratio and decreased p62 protein and mRNA levels. The increase in LC3B-II could be due to increased autophagosome formation or impaired degradation, whereas p62, an autophagic substrate, shows a continuous decrease, suggesting enhanced rather than blocked autophagic flux. Activation of autophagic flux was further confirmed by TEM observation of numerous autophagosomes, punctate MDC accumulation, and LC3B immunofluorescence. Because p62 also has signal-transduction functions, its degradation can weaken pro-survival pathways, thereby increasing WA cytotoxicity. Notably, HDAC1 overexpression reversed the decrease in p62, suggesting that HDAC1 may "clamp" autophagic flux by transcriptionally repressing certain core autophagy genes or upregulating mTORC1 signaling; after WA relieves this

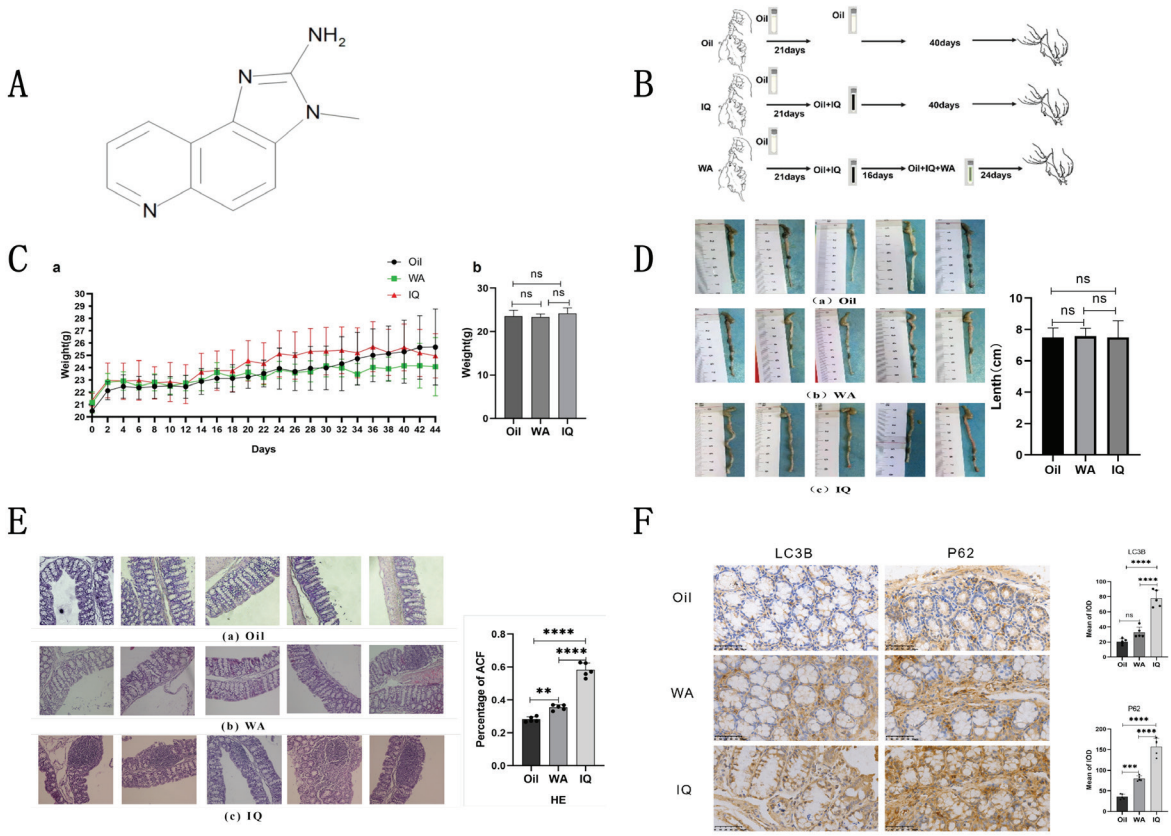

Fig. 6. Structure of IQ (A). Dose and timing of Oil/WA and IQ in different groups (B). Images of mice's dynamic weight (C) and colorectal tissues (D). HE staining showed that the percentage of ACF varied significantly across groups (E). Representative immunohistochemical images and quantitative analyses of LC3B and p62 expression across groups (×200) were also statistically significant (F-test). n=5 mice per group; two-way repeated-measures ANOVA was used for (C), and one-way ANOVA followed by Tukey's post hoc test for (E) and (F). ** $p<0.01$, *** $p<0.001$, **** $p<0.0001$. IQ: 2-amino-3-methyl-3H-imidazo[4,5-f]quinoline; WA: Withaferin-A.

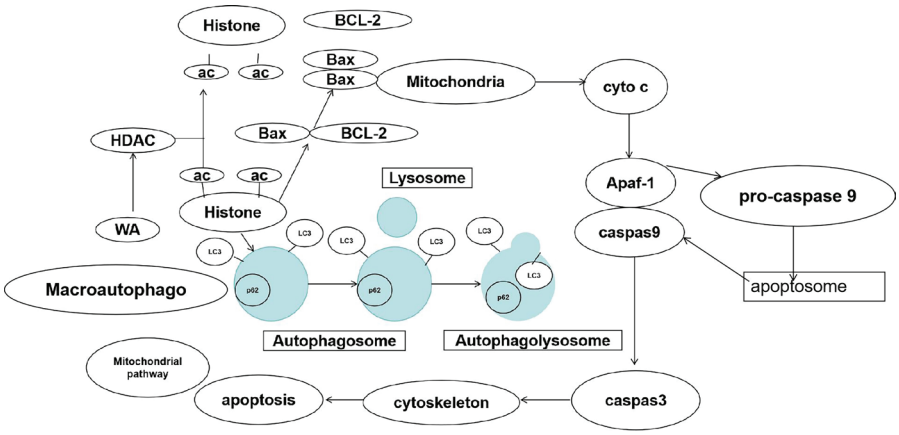

Fig. 7. Mechanism diagram

WA: Withaferin-A, HDAC: Histone deacetylase, Ac: Acetylation, LC3: microtubule-associated protein 1 light chain 3, BCL-2: B cell lymphoma/leukemia-2 protein, Bax: Bcl-2-associated X protein, p62: ubiquitin-binding protein p62.

"clamp," autophagosome formation accelerates along with degradation, leading to p62 consumption. An increased Bax/Bcl-2 ratio is a classic mitochondrial apoptosis switch. HDAC1 binds to the transcriptional repression complex Sin3A/CoREST to deacetylate histone H3K9 at the Bax gene promoter and inhibit transcription; simultaneously, HDAC1 can deacetylate non-histone proteins, thereby weakening their pro-apoptotic functions [14]. Following HDAC1 inhibition by WA, acetylation levels at the Bax promoter region are restored, and transcription is enhanced. Bcl-2 is then downregulated due to the loss of HDAC1-mediated sustained STAT3 activation, leading to an increased Bax/Bcl-2 ratio, greater mitochondrial outer membrane permeability, cytochrome c release, and activation of the caspase-9/3 cascade [22]. Overexpression of HDAC1 again increased histone deacetylation levels and reversed these effects, supporting the HDAC1-acetyl-Bax/Bcl-2-mitochondrial apoptosis axis as a key mechanism of WA.

As previously described, WA may function like a histone deacetylase inhibitor in CRC cells. Therefore, we hypothesized that WA promotes cancer cell death by inhibiting the epigenetic effects of HDACs [15]. Among these, HDAC1 plays an important role. Subsequent experiments confirmed this: HDAC1 expression was significantly upregulated after transfection with a lentiviral vector and purine screening. HDAC1 mRNA and protein levels were measured by RT-qPCR and Western blotting, and the upregulation ratio differed significantly. The CCK8 assay revealed that the IC_{50} values of the two groups also differed significantly. Cell proliferation and motility/migration in the PCMV-HDAC1 group were significantly higher than in the NC group. The rates of apoptosis and autophagy also differed significantly between the two groups. RT-qPCR and Western blotting verified that the mRNA and total protein expression levels of p62/LC3II/I and Bax/Bcl-2 were statistically significant. Based on these results, we found that the anti-cancer effect of WA against the PCMV-HDAC1 group was significantly lower than against the PCMV-NC group.

Finally, to validate our *in vitro* results, we also examined the effects of WA in C57BL/6J mice. The IQ-induced inflammatory CRC model was characterized by a spike in ACF numbers, increased LC3B speckles, and cytoplasmic accumulation of p62 as the main pathological features. After WA treatment, the number of ACFs decreased by more than 60%, and p62/LC3B levels in intestinal tissue decreased significantly. It is important to note that the body weight curve of WA-treated mice was similar to that of the control group, indicating that WA is safe at effective doses and provides a solid basis for its potential future use as an HDAC1-targeted CRC chemopreventive or adjuvant therapy.

This novel treatment may offer a strategy for CRC treatment. In addition to the previously mentioned detection of HDAC1 expression, WA could also inhibit other HDACs in CRC cells. Acetylation of histones can serve as specific anchors for recruiting transcription factors. Finding downstream transcription factors may further elucidate the anti-cancer mechanism of WA. A mechanism diagram is shown in Fig. 7.

These results demonstrate that WA can inhibit CRC cell proliferation and migration. The treatments also decreased Bcl-2 expression and increased Bax expression, thereby elevating the Bax/Bcl-2 ratio. Undeniably, WA enhanced apoptosis in CRC cells. WA also promotes autophagy in CRC cells. Furthermore, we examined the molecular mechanisms underlying WA-induced apoptosis and autophagy in CRC cells. When HDAC1 was overexpressed using a lentiviral vector, all prior effects were abolished. We confirm that these effects are mediated by HDAC1 downregulation. Finally, we tested whether WA had similar effects in CRC cells in vitro. It significantly affected p62 and LC3B levels compared to the oil and IQ groups. The animal model yielded similar results.

Although this study offers initial evidence for the anticancer effects of WA in colorectal cancer and indicates that these effects may be mediated through HDAC1-dependent regulation of apoptosis and autophagy, further research using more diverse experimental models, detailed mechanistic studies, and thorough safety assessments is essential to advance its clinical application. Only Caco-2 and HT-29 cell lines were used in vitro, and their molecular characteristics and drug responses may differ from those of primary tumor cells or patient-derived organoids (PDOs). Additionally, the mouse ACF model only represents the early stage of carcinogenesis, and the effectiveness of WA on established tumors has not been evaluated. Therefore, it is crucial to further verify the safety window, optimal dose, and pharmacokinetic properties of WA using primary cultures, PDO/PDX models, and larger-animal studies, providing a foundation for early clinical trials. Future research should identify the specific molecular targets of WA, explore combination therapies, and perform preclinical pharmacokinetic evaluations to determine the feasibility of WA as a candidate for colorectal cancer prevention and treatment.

This study demonstrated, in both in vitro and in vivo models, that WA decreases HDAC1 expression while promoting apoptosis and autophagy in human colorectal cancer cells. This process inhibits cell proliferation, migration, and colony formation, and significantly reduces IQ-induced ACF in mice. These findings support further development of WA as a chemopreventive or adjunct therapy for colorectal cancer. Since WA did not cause weight loss or overt toxicity in mice at effective doses, and its molecular target, HDAC1, is often overexpressed in patients with colorectal cancer, WA seems to be a promising, low-toxicity, epigenetically targeted oral drug candidate.

Funding

This work received no funding support.

Ethical approval

This study was conducted following the principles of the Declaration of Helsinki. Approval was received from the Laboratory Animal Ethical and Welfare Committee of Shandong University Qilu College of Medicine (Approval number: 21099).

Consent to participate

Informed consent was secured from all participants involved in the study.

Competing interests

The authors have no relevant financial or non-financial interests to disclose.

ORCID numbers of authors

- Qiong Wang (QW): 0000-0003-1561-7559
- Caixia Li (CL): 0009-0003-4741-0429

Author contributions

Both authors contributed to the study's conception and design, participated in data collection, and reviewed and edited the manuscript. Both authors read and approved the final version.

REFERENCES

1. **Puspitaningtyas H, Wiranata JA, Wiratama BS, Fachiroh J, Hutajulu SH.** Association of Low Educational Attainment and Higher Colorectal Cancer Risk: Mediatory Effect of Lifestyle-Associated Factors Within Local Context. World J Oncol. 2025; 16(4):388-396. *https://doi.org/10.14740/wjon2599.*
2. **Huang P, Guo K, Tu J, Fang J, Zhou L, Luo X, et al.** Single-Cell RNA Sequencing Reveals LEF1 as a Prognostic Biomarker for Poor Outcomes in Oxaliplatin-Resistant Colorectal Cancer. Hum Mutat. 2025; 2025:6705599. https://doi.org/*10.1155/humu/6705599.*

3. **Shen R, Cheng F, Guo R, Wang W, Yang X, Chen Y, et al.** Dehydroleucodine exerts an antiproliferative effect on human Burkitt's lymphoma Daudi cells via SLC7A11-mediated ferroptosis. Front Pharmacol. 2025; 16:1572364. https://doi.org/*10.3389/fphar.2025.1572364*.
4. **Wu HC, Tsai CC, Hsu PC, Kuo CY.** Herbal Medicine in Breast Cancer Therapy: Mechanisms, Evidence, and Future Perspectives. Curr Issues Mol Biol. 2025; 47(5):362. https://doi.org/*10.3390/cimb47050362*.
5. **Lee J, Seo Y, Roh JL.** Emerging Therapeutic Strategies Targeting GPX4-Mediated Ferroptosis in Head and Neck Cancer. Int J Mol Sci. 2025; 26(13):6452. https://doi.org/*10.3390/ijms26136452*.
6. **Chen X, Ma X, Hu X, Wang C, Zhang X, Yan C.** Mechanisms and potential therapeutic strategies of withaferin A in breast cancer. Pharmacol Rep. 2025; 77: 1163-1176. https://doi.org/*10.1007/s43440-025-00736-3*.
7. **Heyninck K, Lahtela-Kakkonen M, Van der Veken P, Haegeman G, Vanden Berghe W.** Withaferin A inhibits NF-kappaB activation by targeting cysteine 179 in IKKβ. Biochem Pharmacol. 2014; 91(4):501-509. https://doi.org/*10.1016/j.bcp.2014.08.004*.
8. **Choi BY, Kim BW.** Withaferin-A Inhibits Colon Cancer Cell Growth by Blocking STAT3 Transcriptional Activity. J Cancer Prev. 2015; 20(3):185-192. https://doi.org/*10.15430/JCP.2015.20.3.185*.
9. **Yan Z, Guo R, Gan L, Lau WB, Cao X, Zhao J, et al.** Withaferin A inhibits apoptosis via activated Akt-mediated inhibition of oxidative stress. Life Sci. 2018; 211:91-101. https://doi.org/*10.1016/j.lfs.2018.09.020*.
10. **Mirza S, Sharma G, Parshad R, Gupta SD, Pandya P, Ralhan R.** Expression of DNA methyltransferases in breast cancer patients and to analyze the effect of natural compounds on DNA methyltransferases and associated proteins. J Breast Cancer. 2013;16(1):23-31. https://doi.org/*10.4048/jbc.2013.16.1.23*.
11. **Duan N, Hu X, Qiu H, Zhou R, Li Y, Lu W, et al.** Targeting the E2F1/Rb/HDAC1 axis with the small molecule HR488B effectively inhibits colorectal cancer growth. Cell Death Dis. 2023; 14(12):801. https://doi.org/*10.1038/s41419-023-06205-0*.
12. **Yang Z, Su W, Zhang Q, Niu L, Feng B, Zhang Y, et al.** Lactylation of HDAC1 Confers Resistance to Ferroptosis in Colorectal Cancer. Adv Sci (Weinh). 2025; 12(12):e2408845. https://doi.org/*10.1002/advs.202408845*.
13. **Likasitwatanakul P, Li Z, Doan P, Spisak S, Raghawan AK, Liu Q, et al.** Chemical Perturbations Impacting Histone Acetylation Govern Colorectal Cancer Differentiation. Gastroenterology. 2026; 170(1):70-88. S0016-5085(25)05732-4. https://doi.org/*10.1053/j.gastro.2025.07.003*.
14. **Dhingra N, Gupta V, Tyagi A, Agrawala PK, Gupta V.** Trichostatin A ameliorated combined radiation and skin wound injury-induced mortality and hematopoietic suppression in a rat model. Int J Radiat Biol. 2025; 101(9):952-972. https://doi.org/*10.1080/09553002.2025.2537211*.
15. **Al-Rimawi F, Rishmawi S, Ariqat SH, Khalid MF, Warad I, Salah Z.** Anticancer Activity, Antioxidant Activity, and Phenolic and Flavonoids Content of Wild Tragopogon porrifolius Plant Extracts. Evid Based Complement Alternat Med. 2016; 2016:9612490. https://doi.org/*10.1155/2016/9612490*.
16. **Yang R, Sun S, Zhang Q, Liu H, Wang L, Meng Y, et al.** Pharmacological Inhibition of TXNRD1 by a Small Molecule Flavonoid Butein Overcomes Cisplatin Resistance in Lung Cancer Cells. Biol Trace Elem Res. 2025; 203(4):1949-1960. https://doi.org/*10.1007/s12011-024-04331-0*.
17. **Liu P, Zhang B, Li Y, Yuan Q.** Potential mechanisms of cancer prevention and treatment by sulforaphane, a natural small molecule compound of plant-derived. Mol Med. 2024; 30(1):94. https://doi.org/*10.1186/s10020-024-00842-7*.
18. **An T, Yin H, Lu Y, Liu F.** The Emerging Potential of Parthenolide Nanoformulations in Tumor Therapy. Drug Des Devel

Ther. 2022; 16:1255-1272. https://doi.org/*10.2147/DDDT.S355059.*

19. **Vidjeyamannane C, Joy A, Prakash K, Saravanakumar R.** A comprehensive review on the role of plant-derived bioactive metabolites driving ROS-mediated apoptosis in cancer. Med Oncol. 2025; 42(9):420. https://doi.org/*10.1007/s12032-025-02985-x.*
20. **Wang H, Gu B, Wang Z, Zhang X, Shan L, Liu L, et al.** Emodin enhances host antiviral immunity against Micropterus salmoides rhabdovirus by activating RLR signaling in largemouth bass. Fish Shellfish Immunol. 2025; 166:110633. https://doi.org/*10.1016/j.fsi.2025.110633.*
21. **Dzięgielewska M, Tomczyk M, Wiater A, Woytoń A, Junka A.** Targeting Ocular Biofilms with Plant-Derived Antimicrobials in the Era of Antibiotic Resistance. Molecules. 2025; 30(13):2863. https://doi.org/*10.3390/molecules30132863.*
22. **Lee K, Lee D, Kim JY, Shim JJ, Bae JW, Lee JH.** Attenuation Effect of Withania somnifera Extract on Restraint Stress-Induced Anxiety-like Behavior and Hippocampal Alterations in Mice. Int J Mol Sci. 2025; 26(15):7317. https://doi.org/*10.3390/ijms26157317.*
23. **Albalawi AA.** Dual impact of Ashwagandha: Significant cortisol reduction but no effects on perceived stress - A systematic review and meta-analysis. Nutr Health. 2025; *31(4):1395-1408.* https://doi.org/*10.1 177/02601060251363647.*
24. **Elzayat EM, Elsamahy GE, Mansour GH, El-Sherif AA, Hassan N.** The Synergistic and Anticancer Potential of Withania Somnifera (Ashwagandha) Ethanol Extract as an Adjuvant with Doxorubicin in MCF7 Breast Cancer Cell Line. Asian Pac J Cancer Prev. 2025; 26(3):757-766. https://doi.org/*10.31557/APJCP.2025.26.3.757.*
25. **Baghel K, Azam Z, Srivastava R.** Dietary restriction-induced alterations on estrogen receptor alpha expression in regulating fertility in male Coturnix coturnix japonica: Relevance of Withania somnifera in modulation of inflammation and oxidative stress in testis. Am J Reprod Immunol. 2024; 91(2): e13816. https://doi.org/*10.1111/aji.13816.*
26. **White PT, Subramanian C, Motiwala HF, Cohen MS.** Natural Withanolides in the Treatment of Chronic Diseases. Adv Exp Med Biol. 2016; 928:329-373. https://doi.org/*10.1007/978-3-319-41334-1_14.*
27. **Hameed H, Afzal M, Khan MA, Javaid L, Shahzad M, Abrar K.** Unraveling the role of withanolides as key modulators in breast cancer mitigation. Mol Biol Rep. 2025; 52(1):331. https://doi.org/*10.1007/s11033-025-10442-1.*